Petroleum Science 23 (2026) 2075–2085

Contents lists available at ScienceDirect

Petroleum Science

journal homepage: www.keaipublishing.com/en/journals/petroleum-science

Original Paper

Gelation and reservoir conformance control performance of *in situ* crosslinked polymer gels prepared with different crosslinkers

Ying-Qi Gao, Hong-Bin Cheng, Guan-Hao Li, Hong-Yu Li, Hong-Gen Tan, Jiong Zhang, Dao-Yi Zhu *

China University of Petroleum-Beijing at Karamay, Karamay, 834000, Xinjiang, China

ARTICLE INFO

Article history:
Received 21 October 2025
Received in revised form
5 January 2026
Accepted 6 January 2026
Available online 9 January 2026

Edited by Yan-Hua Sun

Keywords:
In situ crosslinked polymer gel
Crosslinker type
Gel strength
Conformance control
Nuclear magnetic resonance

ABSTRACT

In situ crosslinked polymer gels (ISCPGs) are widely applied in petroleum reservoirs for conformance control and water shutoff to improve oil recovery. However, the differences in gelation behavior and conformance control performance among ISCPGs formulated with different types of crosslinkers, as well as the underlying microscopic mechanisms, remain insufficiently understood. In this study, the gelation properties of three commonly used crosslinkers—chromium (Cr), phenol-formaldehyde (PF) system, and polyethyleneimine (PEI)—with partially hydrolyzed polyacrylamide (HPAM) were evaluated using the Sydansk bottle-testing method. Core displacement experiments were conducted to compare the injectivity and plugging performance of these ISCPGs in both homogeneous and fractured cores. Results show that Cr-ISCPG had the shortest gelation time (0.3–4 h) and the highest gel strength, reaching grade G, but its long-term thermal stability was relatively poor under reservoir conditions (e.g., 73 °C). PF-ISCPG exhibited superior thermal stability, maintained up to 90 d, but had weaker wall-building capacity compared with Cr-ISCPG. PEI, as a biologically and environmentally friendly crosslinker, yielded PEI-ISCPGs with the longest gelation times and thermal stability, also with the best wall-building performance among the three. In homogeneous cores with gas-measured permeability above 500×10^{-3} μm^2, Cr-ISCPG demonstrated strong plugging capability, largely due to its high wall-building strength on rock surfaces. Nuclear magnetic resonance (NMR) analysis provided microscopic insights into ISCPG injection and propagation mechanisms, showing that excessively prolonged gelation time can cause matrix damage. Owing to its stronger wall-building capacity, Cr-ISCPG performed better in plugging highly conductive channels such as fractures, thereby achieving more pronounced conformance control. This work clarified performance differences among ISCPGs crosslinked by different crosslinkers, providing valuable guidance for optimal crosslinker selection and conformance control design in field applications.

1. Introduction

Many mature oilfields worldwide have long entered the high-water-cut development stage, where declining waterflood efficiency has exacerbated ineffective water recycling problems (Song et al., 2024; Yu et al., 2022). In continental sedimentary reservoirs, heterogeneity is typically more pronounced, resulting in generally low waterflood sweep efficiency, thus demanding effective conformance control technologies to improve oil recovery (Al Brahim et al., 2022; Song et al., 2022; Yang et al., 2025). Chemical conformance control agents, owing to their high tunability and large effective treatment radius, have become key tools for profile control and water shutoff to increase oil production (Liu et al., 2022; Seright and Brattekas, 2021). Among these, *in situ* crosslinked polymer gels (ISCPGs) can form three-dimensional (3D) network structures directly within the reservoir, enabling plugging of higher-permeability channels and redirecting subsequent displacement fluids toward previously unswept lower permeability zones (Aldhaheri et al., 2023; Bai et al., 2015; Shamlooh et al., 2022). Nevertheless, the type of crosslinker exerts a

* Corresponding author.
E-mail address: chutaoi@163.com (D.-Y. Zhu).
Peer review under the responsibility of China University of Petroleum (Beijing).

https://doi.org/10.1016/j.petsci.2026.01.003

significant impact on the gelation and plugging performance of ISCPGs, directly influencing the success rate of oilfield applications (Bai et al., 2022). Therefore, a systematic investigation into the performance differences among ISCPGs with different crosslinkers is of substantial scientific and engineering value for achieving successful conformance control.

Industrial crosslinkers currently in use can generally be classified into three categories: metallic ion types, organic synthetic types, and environmentally friendly crosslinkers (Wang et al., 2024; Zhu et al., 2017a). Chromium (Cr), as typical metallic crosslinkers, coordinate with the carboxyl groups of hydrolyzed polyacrylamide (HPAM) to form 3D network structures. Cr-ISCPGs are characterized by rapid gelation times (2–6 h) and high gel strength, but pose heavy-metal pollution risks (Bartosek et al., 1994; Sun et al., 2021; Sydansk, 1988; Zhang et al., 2020). Phenol-formaldehyde (PF) crosslinkers condense hydroxymethyl groups with the amide groups of HPAM to form covalent crosslinked networks (Zhu et al., 2019), resulting in excellent thermal stability (up to 120 °C), though they may release formaldehyde. Polyethyleneimine (PEI), as an environmentally friendly crosslinker, reacts through nitrogen-transfer addition between its primary/secondary amine groups and the carboxyl groups of HPAM, offering biodegradability and salt tolerance (Amir et al., 2022; Reddy et al., 2003; Zhu et al., 2024). These three crosslinkers differ in reaction kinetics, environmental compatibility, and cost-effectiveness, yet their microscale mechanisms of influence on gel injection and plugging in both matrix and fractured cores have not been systematically compared to date.

Existing studies mostly focus on the optimization and evaluation of a single type of ISCPG (Zhu et al., 2017a). Yang et al. (2019) investigated the water-plugging performance of organic chromium based ISCPG in high-salinity formations. Due to the introduction of organic acids, the crosslinking reaction time between chromium and HPAM was extended. Experiments in the sand-packs with permeability of 2864 $\times$ 10^{-3} μm^2 achieved a plugging efficiency as high as 98.4%. They found that polymer aggregates may adhere to the rock surface, which could influence gel strength. Sun et al. (2021) studied the CO_2 breakthrough control using Cr-ISCPGs in Berea cores with permeabilities from 107 $\times$ 10^{-3} to 1225 $\times$ 10^{-3} μm^2 and found that Cr-ISCPGs exhibit high plugging pressure in low-permeability cores. Although chromium is toxic to some extent, it is still widely applied in conformance control and water-plugging operations (Brattekås and Seright, 2023). Zhu et al. (2017b, 2019) investigated the application of PF-ISCPGs in high-temperature reservoirs. The crosslinking reaction between phenol resin and HPAM forms covalent bonds through a dehydration-condensation process, which gives the resulting ISCPG strong thermal resistance, suitable for conformance control in petroleum reservoirs at 150 °C. They mainly used single cores to evaluate the selected single ISCPGs. Albonico et al. (1995) found that, when PF-ISCPGs are injected into the formation, phenol in the composition undergoes chromatographic separation, affecting gelation performance and plugging strength. Lenji et al. (2018) compared four different crosslinkers—PEI-ISCPGs, Al (aluminum)-ISCPGs, PEI-ISCPGs, and PF-ISCPGs—at 90 °C, focusing on the impact of crosslinker type on gelation time and gel rheology. They also found that PEI-ISCPGs and Cr-ISCPGs have higher deformation resistance than PF-ISCPGs. Lei et al. (2022) reviewed the types and characteristics of polymer gels but did not analyze differences in gelation performance and plugging strength among ISCPGs prepared with different crosslinkers.

It is noteworthy that the current evaluation methods have obvious limitations—traditional bottle-testing and rheological measurements can only characterize the bulk gel properties, while core-flooding experiments mostly focus on macro parameters such as plugging efficiency, lacking microscopic interpretation of the dynamic behavior of ISCPGs in porous media (Zhu et al., 2025). Few studies have analyzed performance differences among various crosslinkers using both core-scale and microscopic characterization techniques. This study introduces low-field nuclear magnetic resonance (LF-NMR) technology, in which the T_2 relaxation spectrum can quantitatively characterize the distribution of ISCPGs within cores: signals in the short T_2 region reflect the retention of ISCPG in micropores, whereas signals in the long T_2 region correspond to structural features in large pore channels (Bai et al., 2023; Deng et al., 2022; Zhu et al., 2021). Combined with pressure-difference curve analysis from core displacement experiments, this approach can innovatively compensate for the limitation of existing evaluations based solely on breakthrough pressure gradients.

In this work, three typical crosslinkers—chromium (Cr), phenol-formaldehyde resin (PF), and polyethyleneimine (PEI)—were selected. A multi-scale experimental method was applied to analyze the ISCPGs formed by these crosslinkers. The experimental conditions were selected according to the reservoir conditions of Blocks 7 and 8 in the Xinjiang Oilfield, mainly because ISCPG treatments had been applied there for decades and had achieved many successful results. Different types of crosslinkers had also been applied in the oilfield. Gelation time and gel strength were determined using the Sydansk bottle-testing method. Homogeneous and fractured core-flooding experiments were designed to compare ISCPG injectivity and plugging efficiency. LF-NMR was employed to study the evolution of T_2 distribution of ISCPGs inside the cores. This facilitated the analysis, at the microscopic scale, of the plugging mechanisms of different types of ISCPGs in microscopic pores. By clarifying the strengths and weaknesses of ISCPGs of different types, criteria for crosslinker selection were provided. The findings can theoretically reveal the mechanism by which crosslinker influences conformance performance , and can practically guide the opyimal design of ISCPGs for oilfield applications.

2. Experimental materials and methods

2.1. Experimental materials

The experimental chemicals included sodium chloride (NaCl, AR, 99.5%), sodium bicarbonate ($NaHCO_3$, AR, ≥99.5%), anhydrous magnesium chloride ($MgCl_2$, CP, 99%, powder), anhydrous calcium chloride ($CaCl_2$, AR, 99%), anhydrous sodium carbonate (Na_2CO_3, AR, ≥99.5%), potassium chloride (KCl, AR, ≥99.5%), anhydrous sodium sulfate (Na_2SO_4, AR, ≥99.5%), polyethyleneimine (PEI, 10000 Da, AR, 99%), and heavy water (D_2O, AR, 99.9% D for NMR). All of these reagents were purchased form Shanghai Macklin Biochemical Co., Ltd.

The partially hydrolyzed polyacrylamide (HPAM, 12 million Da, hydrolysis degree 23%), chromium crosslinker (Cr, 30%), and phenol-formaldehyde crosslinker (PF, powder) were supplied by the Xinjiang Oilfield. Deionized water (electrical conductivity less than 0.2 S/cm at 25 °C) was self-prepared. Formation water was prepared by mixing 1000 mL of water (H_2O) or heavy water (D_2O) with 17.38 g of NaCl, 0.42 g of Na_2SO_4, 0.48 g of $NaHCO_3$, 3.53 g of $CaCl_2$, 3.51 g of $MgCl_2{\cdot}6H_2O$, and 0.48 g of KCl. In the static evaluation, water (H_2O) was used during the preparation of ISCPG and the water-saturation stage of the displacement experiment. Heavy water (D_2O) was used for ISCPG preparation and for the secondary waterflood during the core displacement experiment. The cores were artificial sandstone cores with permeability ranging from 50 $\times$ 10^{-3} to 5000 $\times$ 10^{-3} μm^2, provided by Beijing Yuanyang Huanyu Technology Co., Ltd. The detailed parameters are shown in Table 1.

Table 1
Physical properties of sandstone cores.

Core No.	Permeability, 10^{-3} μm^2	Diameter, mm	Length, mm	Porosity, %	Remarks
50-1	50	25.37	70.47	19.38	Cr-ISCPGs
100-1	100	25.12	70.42	19.68	
500-1	500	25.24	69.54	20.10	
1000-1	1000	25.06	69.35	20.45	
5000-1	5000	25.14	70.47	32.38	
50-2	50	25.37	70.74	19.42	PF-ISCPGs
100-2	100	25.13	70.51	19.64	
500-2	500	25.25	69.19	20.07	
1000-2	1000	25.25	69.34	20.47	
5000-2	5000	25.13	70.34	31.86	
50-3	50	25.40	70.20	19.21	PEI-ISCPGs
100-3	100	25.15	70.51	19.69	
500-3	500	25.22	69.19	19.65	
1000-3	1000	25.10	69.34	20.73	
5000-3	5000	25.16	70.34	32.16	

2.2. Preparation of polymer gelant

The ISCPG gelant was composed of HPAM combined with different concentrations of chromium (Cr), phenol-formaldehyde (PF), and polyethyleneimine (PEI), respectively. A total of 3.5 g of solid HPAM particles was slowly added to 1,000 mL of formation water (H_2O or D_2O). Water (H_2O) was used for the static evaluation of ISCPG, while heavy water (D_2O) was used for the gel preparation in core displacement experiments. During addition to the beaker, a magnetic stirrer was used to stir the solution rapidly at a speed of 400±20 rpm for 4 h. The HPAM solution prepared for this experiment had a concentration of 0.35%. Then, a certain amount of the above different types of crosslinkers was added to the polymer solution to obtain gelants of different ISCPGs.

2.3. Sydansk bottle test of ISCPGs

The prepared ISCPG was placed in test tubes, with each tube containing 25 mL of gelant. After capping, the tubes were placed in a thermostatic blast drying oven at 73 °C, allowing the crosslinking reaction between different types of crosslinkers and HPAM to occur. In this study, the Sydansk bottle-testing method was primarily used (Sydansk, 1988; Zhu et al., 2017b). As shown in Fig. 1, the gelation dynamics were determined by observing changes in gel state over time. Based on the different flow states, suspension states, and “tonguing” behavior, the gels were classified into nine grades. The time at which the gel strength in the tube reached Grade D was defined as the gelation time.

2.4. Core displacement experiment

The core displacement experimental method was used to measure core permeability, porosity, and conformance control performance of ISCPG, as shown in Fig. 2.

The specific steps were as follows:

(1) Measurement of core parameters

Artificial cores were placed in a drying oven at 105 °C and dried until their weight no longer changed. Their length, diameter, and dry weight were then measured.

(2) Core water saturation

The cores were vacuumed with a vacuum pump for 6–8 h, then saturated with formation water (H_2O), and weighed to obtain the wet weight. The pore volume (PV) and porosity were calculated,.

(3) Measurement of core permeability

Simulated formation water was injected at a constant rate of 0.5 mL/min. The injection-end pressure was recorded in real time until it became stable.

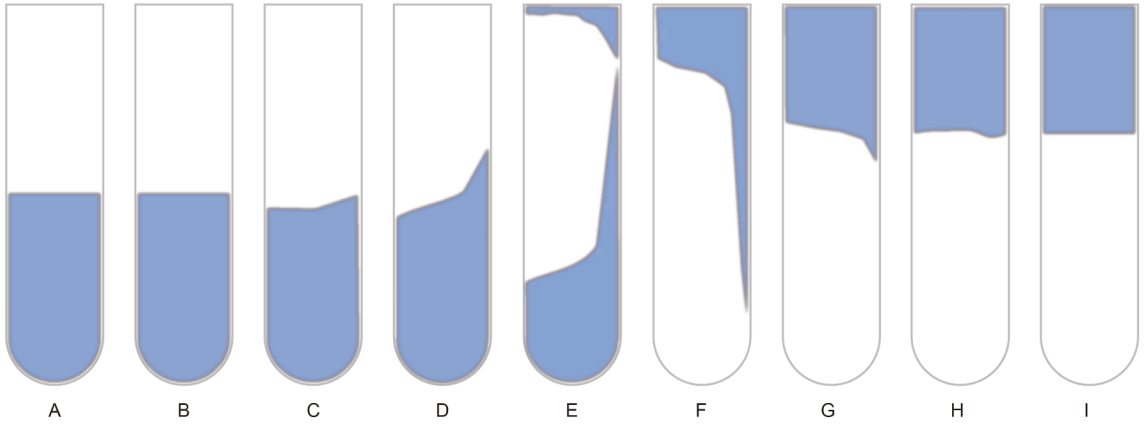

Fig. 1. Schematics of different gel strength codes.

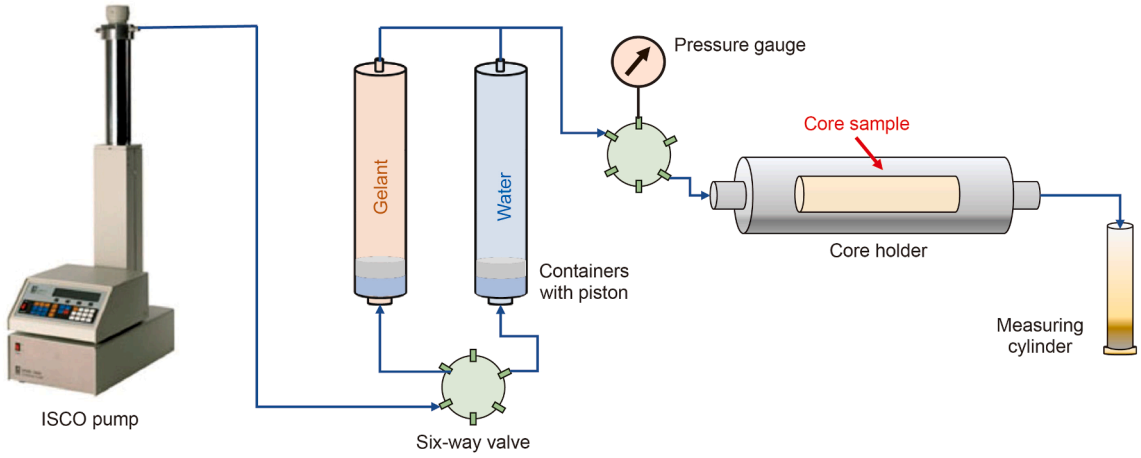

Fig. 2. Schematic diagram of the experimental setup for core displacement.

(4) Gel injection

Gelant prepared by heavy water (D_2O) was poured into the container and injected into cores of different permeabilities at a constant rate of 0.5 mL/min. The pressure was recorded every minute until the injection volume reached 2 PV.

(5) Waiting for gelation

Under simulated reservoir temperature of 73 °C, gel-injected cores were placed in the oven for thermal aging for 3 d.

(6) Secondary heavy-water flooding

Heavy water (D_2O) was injected at a displacement rate of 0.5 mL/min. Displacement pressure and produced liquid volume were recorded every minute. The secondary heavy water (D_2O) flooding was stopped when the pressure stabilized.

(7) Calculation of resistance factor and residual resistance factor

The resistance factor (RF) was calculated using Eq. (1):

$$RF = \frac{\lambda_w}{\lambda_p} = \frac{K_w}{\mu_w} \Big/ \frac{K_p}{\mu_p} \quad (1)$$

where λ_w is the mobility of water, dimensionless; λ_p is the mobility of ISCPG, dimensionless; K_w is the water-measured permeability of core samples, 10^{-3} μm^2; K_p is the permeability of core being injected with ISCPG, 10^{-3} μm^2; μ_w is the viscosity of water, mPa·s; μ_p is the viscosity of ISCPG, mPa·s.

The residual resistance factor (RRF) described the ability of ISCPG to reduce permeability. It was calculated using Eq. (2) as the ratio of the initial water-measured permeability K_w before ISCPG injection to the water-measured permeability K_f during secondary water flooding:

$$RRF = \frac{K_w}{K_f} \quad (2)$$

where K_f is the water-measured permeability during secondary water flooding, 10^{-3} μm^2.

2.5. Core NMR T_2 spectrum measurement

A nuclear magnetic resonance imaging system (SPEC-RC035, Beijing SPEC Company) was used to perform nuclear magnetic resonance (NMR) T_2 analysis of cores. The sampling interval (DW) was set to 2 μs, the number of echoes (NECH) was 4096, the number of scans (SCAN) was 64, the receiver gain (RG) was 20 dB, and the waiting time was 3000 ms. The prepared core samples were measured during ISCPG injection and after the secondary water flooding. The T_2 (transverse relaxation time) spectrum data of the core samples were obtained. By analyzing the signal changes at each stage, the variations of nuclear magnetic hydrogen signals in the core were determined, thereby analyzing the migration behavior of the gelant in the core and the microscopic water-flow channels during the secondary water flooding after ISCPG treatment. It is worth noting that T_2 was selected instead of T_1 (longitudinal relaxation time) mainly because T_2 measurement was simpler and faster, and it could reflect the pore-structure characteristics of the rock.

3. Results and discussion

3.1. Gelation performance of ISCPGs with different crosslinkers in bottle tests

Before the core displacement experiments, the static gelation performance of ISCPGs with different crosslinkers was evaluated using the bottle-testing method. For all three types of ISCPGs, the HPAM concentration was 0.35%, and the crosslinker concentration is shown in Table 2. Under a temperature of 73 °C, the Sydansk bottle-testing method described in Section 2.3 was used to evaluate gelation performance. The gelation time was determined when the Sydansk gel strength reached Grade D. The experimental results are shown in Table 2.

From Table 2, the data clearly revealed distinct characteristics of the three crosslinkers. Cr-ISCPG showed a fast gelation rate and high gel strength, forming a rapid, strong gel suitable for near-wellbore plugging. However, its thermal stability was poor, remaining stable for only 1 d. Cr-ISCPG might dehydrate quickly and was not suitable for operations requiring long-term stability. It might be applicable only for short-term, strong plugging in the near-wellbore zone and not for deep conformance control. PF-

Table 2
Comparison of gelation performance of HPAM with different crosslinkers in bottle tests.

Gel No.	HPAM concentration, %	Crosslinker type	Crosslinker concentration, %	Gelation time, h	Gel strength	Wall-adhesion	Thermal stability, d
A-1	0.35	Cr	0.025	24.0	Grade D	Strong	10
A-2	0.35	Cr	0.150	0.5	Grade F	Strong	1
A-3	0.35	Cr	0.250	0.3	Grade G	Strong	1
B-1	0.35	PF	0.300	6.0	Grade D	Weak	60
B-2	0.35	PF	0.350	4.0	Grade E	Weak	90
B-3	0.35	PF	0.400	2.0	Grade E	Weak	60
C-1	0.35	PEI	0.300	72.0	Grade E	Relatively strong	120
C-2	0.35	PEI	0.350	48.0	Grade F	Relatively strong	120
C-3	0.35	PEI	0.400	24.0	Grade G	Relatively strong	120

ISCPG exhibited a moderate gelation rate, medium gel strength, weak wall-adhesion, and thermal stability of 60–90 d. It met the duration requirements of most conformance control operations. Although it had potential for deep displacement, its plugging strength might not be high. PEI-ISCPG showed significant delayed-gelation characteristics and finally formed high-strength gels. It had good thermal stability, remaining stable for 120 d, and was suitable for high-temperature reservoirs.

3.2. Conformance control performance of ISCPGs with different crosslinkers in homogeneous cores

3.2.1. Injection performance of ISCPGs with different crosslinkers in homogeneous cores

To evaluate the injection performance of ISCPGs with different crosslinkers in homogeneous cores, the crosslinkers used in the experiments were 0.15% chromium, 0.35% phenol-formaldehyde, and 0.35% PEI. The results are shown in Fig. 3.

From Fig. 3(a), when the core permeabilities were 50×10^{-3}, 100×10^{-3}, 500×10^{-3}, 1000×10^{-3}, and 5000×10^{-3} μm^2, the injection pressure differences during Cr-ISCPG injection at a flow rate of 0.5 mL/min were 4.284, 3.743, 2.337, 1.508, and 1.472 MPa, respectively. As the core permeability increased, the injection pressure of Cr-ISCPG gradually decreased, showing improved injectivity, as shown in Fig. 3(d). The pressure-difference value selected in the figure was the value measured when the injection volume of the gelant reached 2 PV, and it was used for comparison. The matrix permeability of 500×10^{-3} μm^2 (gas-measured) was a critical value for Cr-ISCPG injection. When the permeability decreased to 100×10^{-3} μm^2, gelants exhibited obvious pressure build-up, and all curves maintained an increasing trend. It was mainly because the Cr-ISCPG had a short gelation time and strong wall-adhesion. During injection, Cr-ISCPG gradually accumulated in core pores and had poor transportability, resulting in continuous pressure build-up and poor injectivity, even in cores with permeabilities of 1000×10^3 to 5000×10^3 μm^2.

Fig. 4 shows the resistance factors of ISCPGs prepared with different crosslinkers during injection into cores with different permeabilities. It was noteworthy that the resistance factor showed the opposite trend—when the core permeability increased, the resistance factor also increased. Comparison between the pressure-difference curve and the resistance-factor curve indicated that, even when the injection pressures at permeabilities of 1000×10^{-3} and 5000×10^{-3} μm^2 were below 2 MPa, the resistance factors were 3770 and 4906, respectively, which were high. Therefore, when injecting Cr-ISCPG into the formation, the injection timing needed to be restricted; otherwise, injection would be difficult. In addition, this finding highlighted the necessity of using the resistance factor as an evaluation indicator when testing conformance agents in relatively high permeability cores (1000×10^3 to 5000×10^3 μm^2). Since the pressure build-up after injecting 2 PV did not exceed 3 MPa, injection difficulties did not occur. In contrast, in cores with permeabilities below 500×10^{-3} μm^2, although the resistance factor was lower, the pressure build-up was significantly higher. Therefore, we recommended using the injection pressure difference as the main evaluation indicator.

Fig. 3(b) showed the injection pressure differences of PF-ISCPG. When the core permeabilities were 50×10^{-3}, 100×10^{-3}, 500×10^{-3}, 1000×10^{-3}, and 5000×10^{-3} μm^2, the injection pressures were 7.310, 7.150, 3.143, 0.344, and 0.344 MPa, respectively. As the core permeability increased, the injection pressure of PF-ISCPG gradually decreased, and the injectivity improved. In addition, the gel injection pressure trend was similar to that of Cr-ISCPG, in which a core permeability of 500×10^{-3} μm^2 (gas-measured) was a critical value for PF-ISCPG. When the core permeability decreased to 100×10^{-3} μm^2, the gelants exhibited obvious pressure build-up, which was higher than that of Cr-ISCPG, and finally stabilized. It was mainly because chromium is a heavy-metal ion that caused the polymer molecular chains to shrink, reducing the solution viscosity. Moreover, PF-ISCPG had a higher concentration and formed organic crosslinks, which were less affected by shear. When the core permeabilities were 1000×10^{-3} and 5000×10^{-3} μm^2, the ISCPG injection pressures were below 2 MPa, and the resistance factors were 688 and 123, respectively, which were relatively low. Therefore, compared with Cr-ISCPGs, PF-ISCPGs showed better injectivity in cores with permeabilities below 500×10^{-3} μm^2. However, for permeabilities above 500×10^{-3} μm^2, the injectivity improved during gelation because of continuous dehydration from the gelation reaction.

Fig. 3(c) showed that when the core permeabilities were 50×10^{-3}, 100×10^{-3}, 500×10^{-3}, 1000×10^{-3}, and 5000×10^{-3} μm^2, the gel injection pressures were 3.676, 1.665, 0.275, 0.171, and 0.009 MPa, respectively. As the core permeability increased, the injection pressure of PEI-ISCPG gradually decreased, and the injectivity improved. A core permeability of 100×10^{-3} μm^2 (gas-measured) was a critical value. When the core permeability decreased to 100×10^{-3} μm^2, gelants showed obvious pressure build-up. However, the overall pressures were lower than those of Cr-ISCPG and PF-ISCPG. This was because the gelation time of PEI-ISCPG was slower, and before gelation, the wall-adhesion was weak, allowing injection into cores with permeability as low as 100×10^{-3} μm^2. From Fig. 4, the resistance-factor trend of PEI-ISCPG was similar to that of PF-ISCPG; as the core permeability increased, the resistance factor decreased overall. The strong alkalinity of PEI also reduced the gelant viscosity.

Overall, PEI showed better injectivity. The gel injection pressures under PEI-ISCPG were generally low, all below 2 MPa for core permeabilities of 100×10^{-3}, 500×10^{-3}, 1000×10^{-3}, and 5000×10^{-3} μm^2. The resistance factors were also low, indicating the best plugging performance. Therefore, PEI, as an environmentally friendly crosslinker, had low biotoxicity and good injectivity.

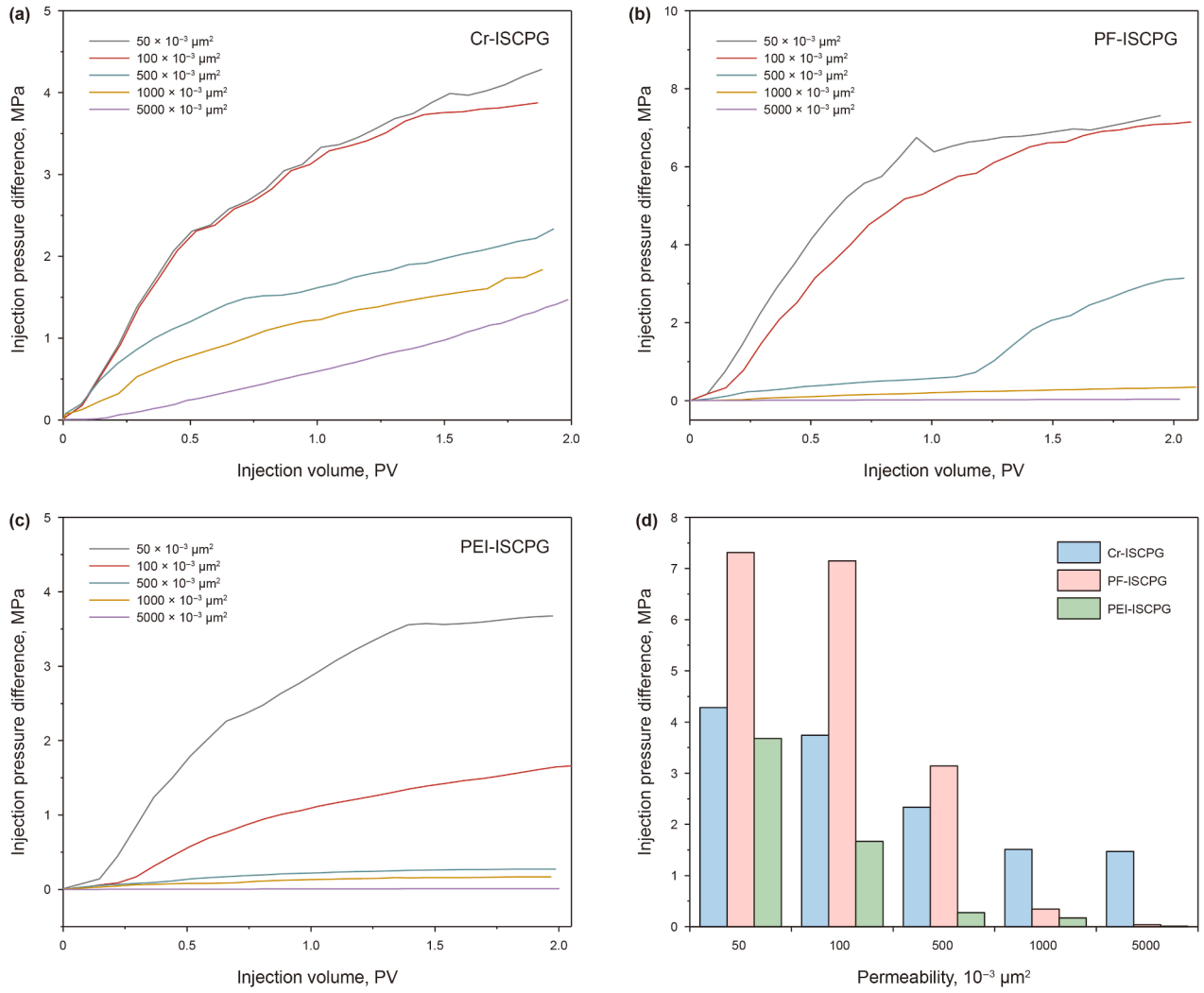

Fig. 3. Comparison of the injection pressure differences of ISCPGs with different crosslinkers in homogeneous cores.

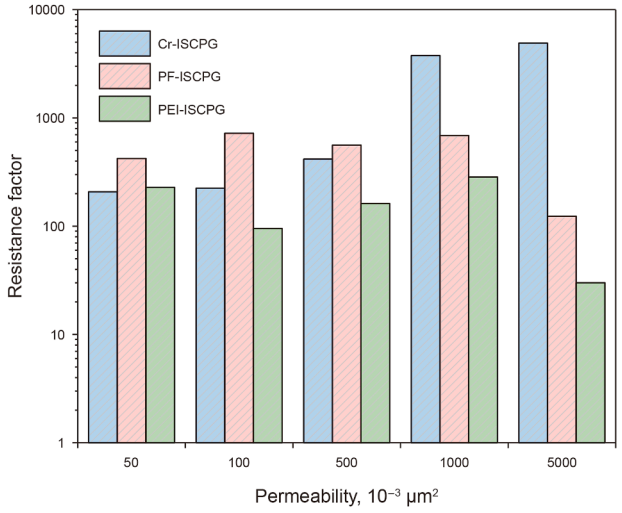

Fig. 4. Comparison of the resistance factor of ISCPGs with different crosslinkers.

3.2.2. *Plugging performance of ISCPGs with different crosslinkers*

To study the plugging performance of ISCPGs with different crosslinkers in homogeneous cores, ISCPG was injected into cores with five matrix permeabilities of 50×10^{-3}, 100×10^{-3}, 500×10^{-3}, 1000×10^{-3}, and 5000×10^{-3} μm^2, respectively. After injection, the cores aged for 3 d at 73 °C. Finally, heavy water was injected into ISCPGs-treated cores at a rate of 0.5 mL/min. The purpose of injecting heavy water was to mask the signal of injected water during the subsequent waterflood (i.e., heavy water) so that the micro-scale sweep performance of the injected water during secondary water flooding (i.e., pore-size distribution) could be analyzed. The pressure change in the core inlets with different matrix permeabilities was recorded, and the residual resistance factor and plugging efficiency were calculated, as shown in Fig. 5.

Fig. 5(a) showed that, for Cr-ISCPG, the plugging performance first increased and then decreased with increasing core permeability during secondary water flooding. A matrix permeability of 500×10^{-3} μm^2 (gas-measured) was a critical value. This was mainly because injection was difficult when the permeability was below 500×10^{-3} μm^2, and plugging occurred only at the core inlet face, with limited plugging strength. When the permeability was above 500×10^{-3} μm^2, the gel strength was limited. Fig. 6 showed the stable pressure and residual resistance factor for different crosslinkers. It could be seen that when the core matrix permeability was greater than 500×10^{-3} μm^2, Cr-ISCPG had the highest stable pressure and residual resistance factor.

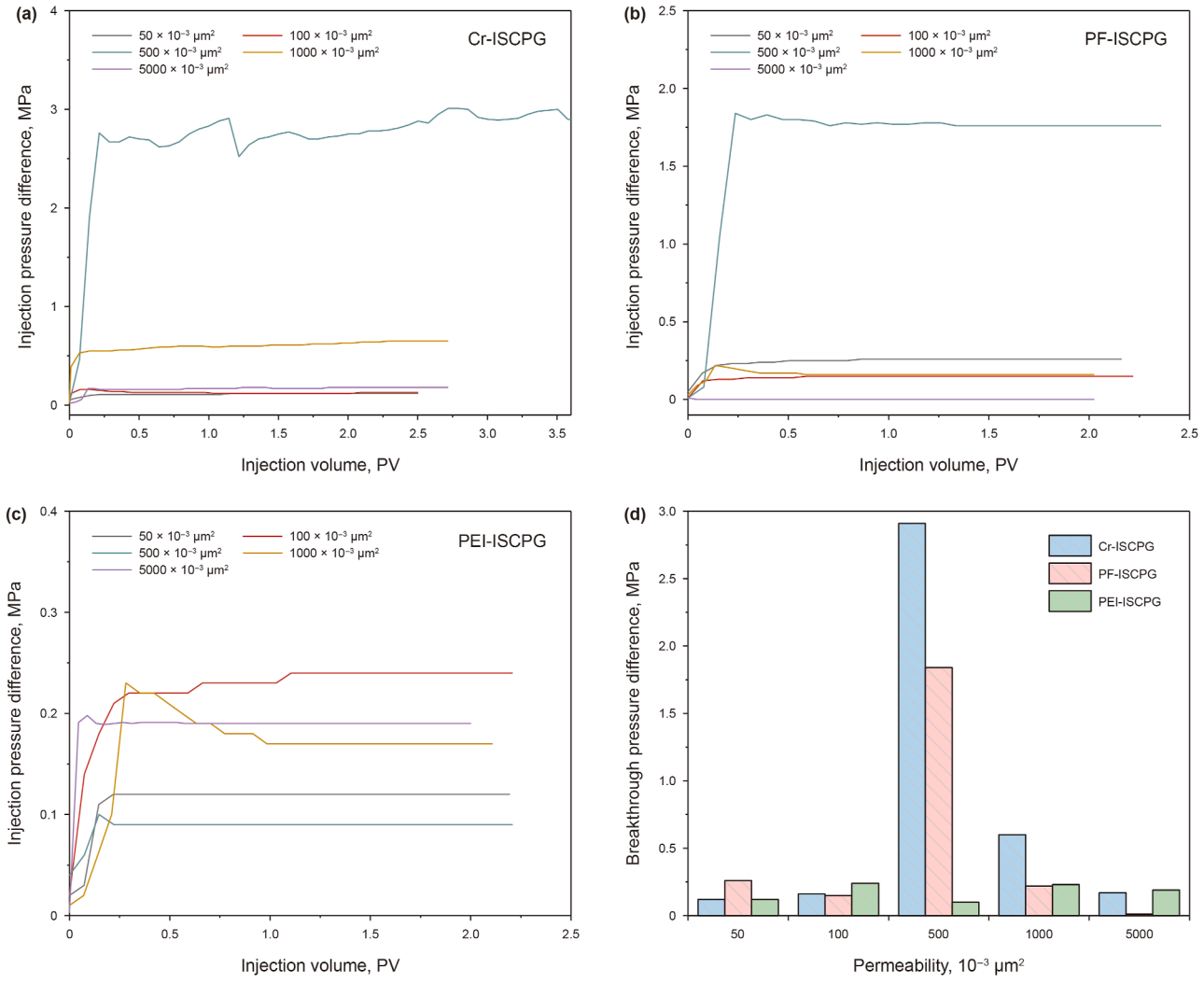

Fig. 5. Injection pressure differences during secondary water flooding after gelation for different ISCPGs with different crosslinkers in homogeneous cores.

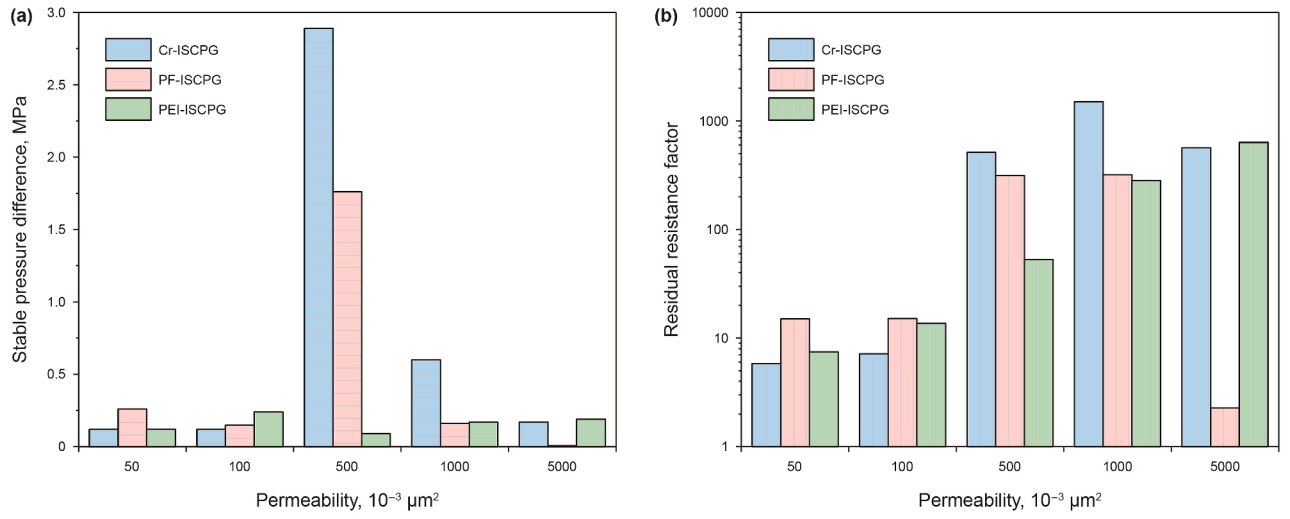

Fig. 6. Stable pressures and residual resistance factors for different ISCPGs with different crosslinkers.

Fig. 7 compared the plugging efficiencies of different ISCPGs in homogeneous cores after gelation. Although the overall plugging efficiencies were high, the plugging pressures were not significant. Therefore, this index was not highly applicable. Resistance factor and residual resistance factor were mainly used for polymer evaluation and were not suitable for ISCPG treatments. The

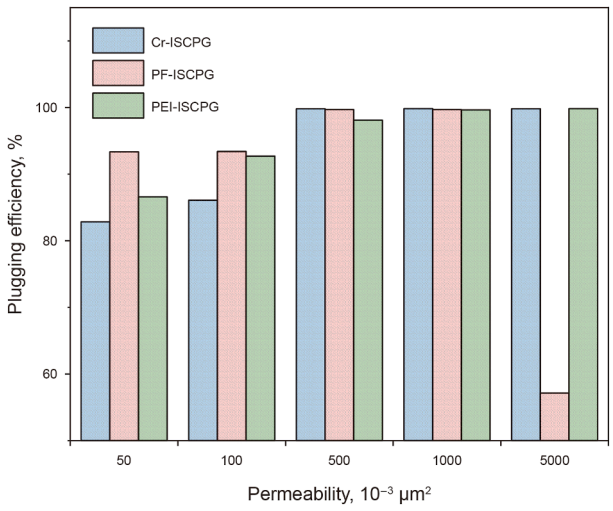

Fig. 7. Plugging efficiencies after gelation for different ISCPGs with different crosslinkers.

residual resistance factor in high-permeability cores showed a clear maximum, indicating that high-strength gels could form certain plugging in high-permeability reservoirs.

Fig. 5(b) showed that, for PF-ISCPG, the plugging performance first increased and then decreased with increasing core permeability. A core permeability of 500×10^{-3} μm^2 (gas-measured) was a critical value. Overall, its performance was lower than that of Cr-ISCPG, mainly because the wall-adhering ability was inferior to Cr-ISCPG. Moreover, dehydration occurred during the reaction, which allowed water channels to form more quickly, resulting in poorer plugging ability. When the core permeability exceeded 5000×10^{-3} μm^2, the plugging performance was essentially negligible. Therefore, PF-ISCPG was not suitable for plugging in reservoirs with permeability greater than 5000×10^{-3} μm^2. Although the plugging efficiency in Fig. 7 was high, the plugging pressure was low, and the plugging performance in homogeneous cores was reduced.

Fig. 5(c) showed that, for PEI-ISCPG, the plugging performance increased with increasing core permeability. A core permeability of 500×10^{-3} μm^2 (gas-measured) was also a critical value. The resistance factor was smaller than that of Cr-ISCPG but better than PF-ISCPG. A smaller resistance factor allowed the gel to migrate farther. In Fig. 7, the plugging efficiency was unexpectedly close to that of Cr-ISCPG; however, the plugging strength was lower than that of Cr-ISCPG. Again, this confirmed that the concept of plugging efficiency was not entirely appropriate, especially when comparing plugging differences among cores with different permeabilities.

3.2.3. Conformance control performance of ISCPGs with different crosslinkers

To clarify the injection and conformance control performance of ISCPGs with different crosslinkers in homogeneous cores, three different ISCPGs (prepared with heavy water) were injected into homogeneous cores of different permeabilities, followed by nuclear magnetic resonance (NMR) testing. The test results are shown in Fig. 8.

When Cr-ISCPG was injected into homogeneous cores, the signal intensity in macropores of 10–1000 ms was greatly reduced. It indicated that Cr-ISCPG moved and was retained more in large pores. However, the signal intensity in small pores of 0–10 ms was higher than that of the other two ISCPG systems. This was mainly because the ISCPG flowed more easily in large pores during migration, and plugging occurred mainly in large pores. Due to the shorter gelation time of Cr-ISCPG, the formed gel was more difficult to enter small pores. When PF-ISCPG and PEI -ISCPG were used, the proportion of small pores swept by heavy water increased significantly. This was because their gelation time was longer than that of Cr-ISCPG. During injection, their higher viscosity produced greater pressure difference, which pushed the gel into smaller pores, resulting in more small-pore plugging. However, this was opposite to the plugging pressure difference trend shown in Fig. 6. That is, the plugging strength of the core was not necessarily related to whether the gel entered more small pores.

In cores with permeability lower than 100×10^{-3} μm^2, the gel was not applicable due to poor injectivity. When the permeability was higher than 500×10^{-3} μm^2, Cr-ISCPG showed stronger wall-attachment ability (stronger interaction with the rock surface), which caused higher plugging pressure difference and thus greater plugging strength. Therefore, ISCPGs were mainly suitable for plugging high-permeability channels. It was worth noting that extending gelation time could cause ISCPGs to be forced into low-permeability layers near high-permeability zones under high injection pressure before and during gelation. This could lead to matrix damage and make the residual oil in small pores more difficult to produce. This was an issue that required attention (Zhu et al., 2025).

3.3. Conformance control performance of ISCPGs with different crosslinkers in fractured cores

3.3.1. Injection and plugging performance of ISCPGs with different crosslinkers

To further evaluate the injection and plugging performance of ISCPGs formed from different crosslinkers in high-thief channels, experiments were conducted using fractured cores with the matrix permeability of 50×10^{-3} μm^2, as shown in Fig. 9. The fracture was supported by uniformly distributed 40–70 mesh ceramic proppant sand, occupying 1/4 of the fracture volume.

As shown in Fig. 9(a), Cr-ISCPG had the highest injection pressure and the shortest gelation time. The PF-ISCPG had a medium injection pressure because of its high initial viscosity. PEI-ISCPG had the lowest pressure due to its lowest initial viscosity. Fig. 9(b) shows the displacement pressure difference during subsequent water injection after gelation in the core. Because Cr-ISCPG and PEI-ISCPG had stronger wall-adhering ability on fracture surfaces, Cr-ISCPG achieved the best plugging performance among the three.

3.3.2. Conformance control performance of ISCPGs with different crosslinkers

To clarify the conformance control performance of different crosslinkers with HPAM in fractured cores, three ISCPGs (prepared with heavy water) were injected into fractured cores, followed by nuclear magnetic resonance (NMR) testing both after ISCPG injection and after secondary water flooding (heavy water). The test results are shown in Fig. 10.

As shown in Fig. 10, because Cr-ISCPG had a shorter gelation time and higher gel strength, the gel (or the water within it) intruded into the matrix during injection, resulting in a significant reduction of signal intensity in both large and small pores. PF-ISCPG had a shorter gelation time than PEI-ISCPG, so the signal intensities in large and small pores also decreased to some extent. After gelation and subsequent secondary water flooding (heavy-water flooding), the T_2 signal of the core injected with PF-ISCPG showed almost no change, whereas the T_2 signal of the core injected with Cr-ISCPG slightly decreased. It was mainly because

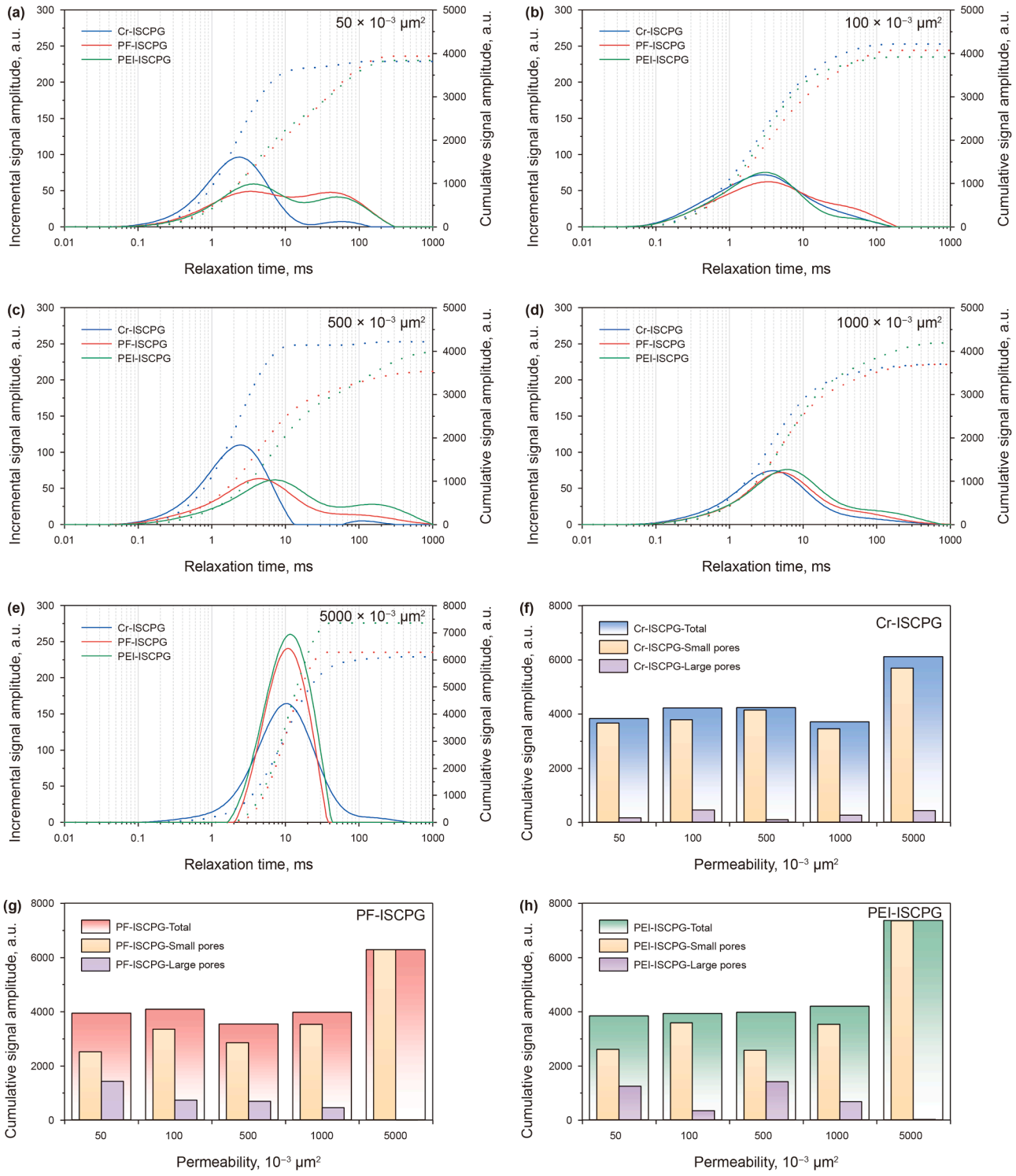

Fig. 8. Variation in NMR signals in cores after reaction of ISCPGs with different crosslinkers followed by secondary heavy-water flooding.

PF-ISCPG had poor wall-adhering ability and less effective plugging in fracture channels. Cr-ISCPG exhibited strong plugging during the injection stage, and heavy water in the gel was already forced into the matrix, leading to minor signal changes. For PEI-ISCPG, the large-pore signal decreased significantly after gelation due to its certain gel strength, and part of the water in large pores was forced into small pores under the pressure difference, resulting in decreased signal in small pores. In summary, Cr-ISCPG provided the best plugging effect for fractures and other high-thief channels.

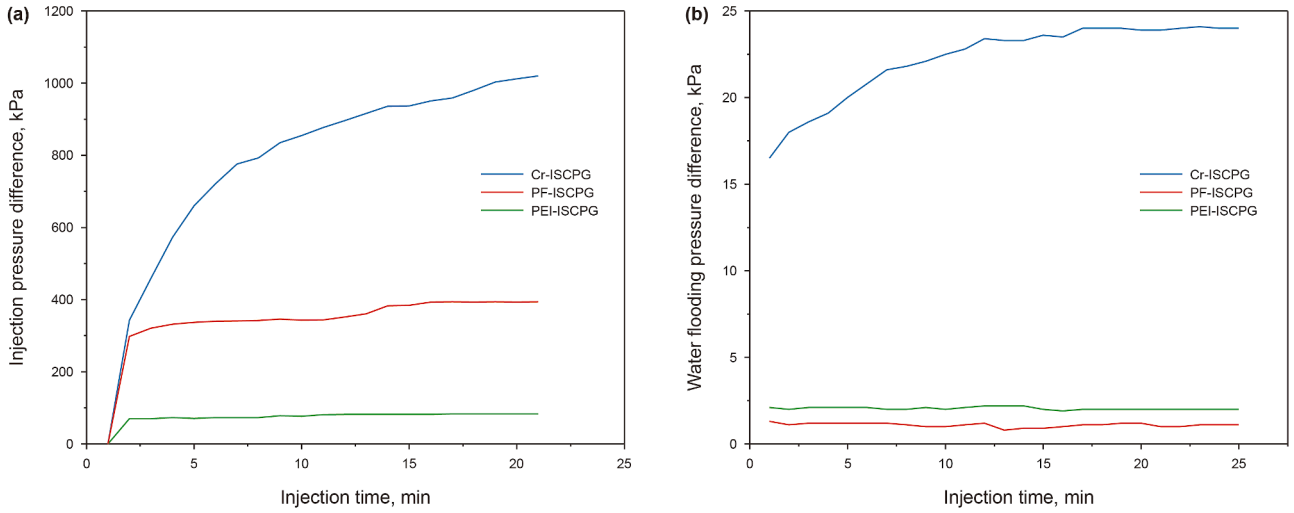

Fig. 9. Comparison of injection pressure differences and secondary water flooding pressure differences for of ISCPGs with different crosslinkers in fractured cores.

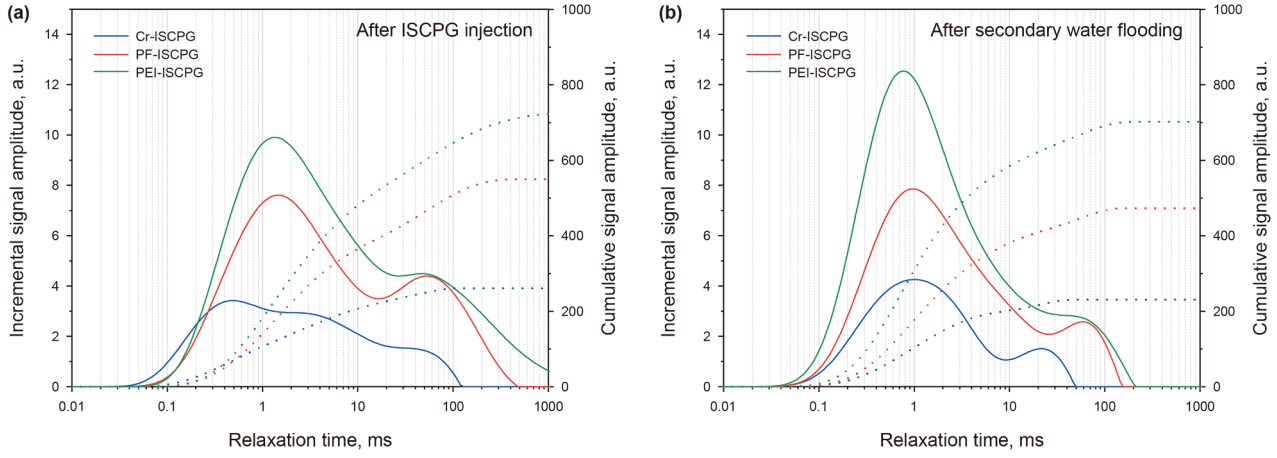

Fig. 10. Comparison of injection and conformance control performance (after secondary water flooding) of ISCPGs with different crosslinkers in fractured cores.

4. Conclusions

Based on displacement experiments and NMR analysis of core samples, this study revealed the differences in injection and plugging performance of *in situ* crosslinked polymer gels (ISCPGs) prepared with different crosslinkers. The main conclusions were as follows:

(1) In the Sydansk bottle-testing method, different crosslinkers with HPAM showed different gelation times, gel strengths, and wall-adhering properties.
(2) In homogeneous cores with permeability below 100×10^{-3} μm^2, all ISCPGs faced injection difficulties and became unsuitable for application.
(3) In homogeneous cores with permeability above 500×10^{-3} μm^2, the Cr-ISCPG showed strong plugging, mainly due to its strong wall-adhering ability on rock surfaces.
(4) The resistance factor and residual resistance factor were not suitable indicators for polymer gel evaluation, because gel formation created a three-dimensional (3D) network structure, and its plugging effect on pores was more critical.
(5) NMR technology analyzed the injection and propagation mechanisms of underground crosslinked gels at the microscopic level. Excessive extension of the gelation time caused matrix damage in cores.
(6) Because of the stronger wall-adhering ability of Cr-ISCPG, it provided better plugging performance in fractures and other high-thief channels, achieving a more effective conformance control.

CRediT authorship contribution statement

Ying-Qi Gao: Writing – original draft, Visualization, Validation, Methodology, Data curation. **Hong-Bin Cheng:** Validation, Methodology, Data curation. **Guan-Hao Li:** Validation, Investigation, Data curation. **Hong-Yu Li:** Validation, Investigation, Data curation. **Hong-Gen Tan:** Validation, Investigation, Data curation. **Jiong Zhang:** Validation, Investigation, Data curation. **Dao-Yi Zhu:** Writing – review & editing, Validation, Supervision, Methodology, Conceptualization.

Declaration of competing interest

The authors declare that they have no known competing financial interests or personal relationships that could have appeared to influence the work reported in this paper.

Acknowledgement

This work was supported by the Oil & Gas Major Project (2025ZD1405006).

References

Al Brahim, A., Bai, B., Schuman, T., 2022. Comprehensive review of polymer and polymer gel treatments for natural gas-related conformance control. Gels 8 (6), 353. https://doi.org/10.3390/gels8060353.

Albonico, P., Bartosek, M., Malandrino, A., Bryant, S., Lockhart, T., 1995. Studies on phenol-formaldehyde crosslinked polymer gels in bulk and in porous media. In: SPE International Conference on Oilfield Chemistry. https://doi.org/10.2118/28983-MS.

Aldhaheri, M., Wei, M., Bai, B., 2023. A systematic design approach for bulk gel treatments based on gel volume-concentration ratio in field projects. Geoenergy Sci. Eng. 221, 211393. https://doi.org/10.1016/j.geoen.2022.211393.

Amir, Z., Saaid, I.M., Mohd Junaidi, M.U., Wan Bakar, W.Z., 2022. Weakened PAM/PEI polymer gel for oilfield water control: Remedy with silica nanoparticles. Gels 8 (5), 265. https://doi.org/10.3390/gels8050265.

Bai, B., Zhou, J., Yin, M., 2015. A comprehensive review of polyacrylamide polymer gels for conformance control. Petrol. Explor. Dev. 42 (4), 525–532. https://doi.org/10.1016/S1876-3804(15)30045-8.

Bai, B., Leng, J., Wei, M., 2022. A comprehensive review of in-situ polymer gel simulation for conformance control. Pet. Sci. 19 (1), 189–202. https://doi.org/10.1016/j.petsci.2021.09.041.

Bai, L., Shi, C.Y., Tang, K., Xie, H., Yang, S.L., 2023. Study on migration and plugging performance of polymer gel in fractured cores using nuclear magnetic resonance technology. Geoenergy Sci. Eng. 227, 211891. https://doi.org/10.1016/j.geoen.2023.211891.

Bartosek, M., Mennella, A., Lockhart, T.P., Causin, E., Rossi, E., Passucci, C., 1994. Polymer gels for conformance treatments: Propagation of Cr(III) crosslinking complexes in porous media. In: SPE Improved Oil Recovery Conference. https://doi.org/10.2118/27828-MS.

Brattekås, B., Seright, R., 2023. A review of polymer gel utilization in carbon dioxide flow control at the core and field scale. SPE J. 28 (6), 3291–3307. https://doi.org/10.2118/217427-PA.

Deng, Z., Liu, M., Qin, J., Sun, H., Zhang, H., Zhi, Keke, Zhu, D.Y., 2022. Mechanism study of water control and oil recovery improvement by polymer gels based on nuclear magnetic resonance. J. Petrol. Sci. Eng. 209, 109881. https://doi.org/10.1016/j.petrol.2021.109881.

Lei, S., Sun, J., Lv, K., Zhang, Q., Yang, J., 2022. Types and performances of polymer gels for oil-gas drilling and production: A review. Gels 8 (6), 386. https://doi.org/10.3390/gels8060386.

Lenji, M.A., Haghshenasfard, M., Sefti, M.V., Salehi, M.B., Moghadam, A.M., 2018. Numerical modeling and experimental investigation of inorganic and organic crosslinkers effects on polymer gel properties. J. Petrol. Sci. Eng. 160, 160–169. https://doi.org/10.1016/j.petrol.2017.10.045.

Liu, J., Almakimi, A., Wei, M., Bai, B., Hussein, I.A., 2022. A comprehensive review of experimental evaluation methods and results of polymer micro/nanogels for enhanced oil recovery and reduced water production. Fuel 324, 124664. https://doi.org/10.1016/j.fuel.2022.124664.

Reddy, B., Eoff, L., Dalrymple, E., Black, K., Brown, D., Rietjens, M., 2003. A natural polymer-based cross-linker system for conformance gel systems. SPE J. 8 (2), 99–106. https://doi.org/10.2118/84937-PA.

Seright, R., Brattekas, B., 2021. Water shutoff and conformance improvement: An introduction. Pet. Sci. 18, 450–478. https://doi.org/10.1007/s12182-021-00546-1.

Shamlooh, M., Elaf, R., Hussein, I.A., Saad, M., Bai, B., 2022. Chitosan/polyacrylamide green gels for water control in high-temperature reservoirs. Energy Fuels 36 (7), 3816–3824. https://doi.org/10.1021/acs.energyfuels.2c00242.

Song, T., Feng, Q., Schuman, T., Cao, J., Bai, B., 2022. A novel branched polymer gel system with delayed gelation property for conformance control. SPE J. 27 (1), 105–115. https://doi.org/10.2118/206742-PA.

Song, T., Bai, B., Huang, R., Zhang, S., Liu, P., Eriyagama, Y., Tian, X., Ahdaya, M., Schuman, T., 2024. Development and evaluation of lysine-crosslinked re-crosslinkable particle gel for water control in high-temperature reservoirs. J. Mol. Liq. 407, 125133. https://doi.org/10.1016/j.molliq.2024.125133.

Sun, X., Bai, B., Alhuraishawy, A.K., Zhu, D., 2021. Understanding the plugging performance of HPAM-Cr (III) polymer gel for CO_2 conformance control. SPE J. 26 (5), 3109–3118. https://doi.org/10.2118/204229-PA.

Sydansk, R.D., 1988. A new conformance-improvement-treatment chromium (lll) gel technology. In: SPE Improved Oil Recovery Conference. https://doi.org/10.2118/17329-MS.

Wang, K., Luo, M., Pu, J., G, C., Li, M., Sun, Z., Pu, C., 2024. Effect and mechanism of zirconium crosslinker on retarding degradation of HPAM/PEI gel system in medium-salinity reservoirs. SPE J. 29 (11), 6516–6529. https://doi.org/10.2118/223597-PA.

Yang, H., Iqbal, M., Lashari, Z., Cao, C., Tang, X., Kang, W., 2019. Experimental research on amphiphilic polymer/organic chromium gel for high salinity reservoirs. Colloids Surf. A Physicochem. Eng. Asp. 582, 123900. https://doi.org/10.1016/j.colsurfa.2019.123900.

Yang, N., Wang, Z., Li, Z., Si, S., Liu, Y., Dai, C., Zhao, G., 2025. Comprehensive displacement system utilizing dispersed particle gels coupling viscosity reduction and breakthrough channel control for heavy oil cold production. Energy Fuels 39 (26), 12449–12461. https://doi.org/10.1021/acs.energyfuels.5c01587.

Yu, B., Zhao, S., Long, Y., Bai, B., Schuman, T., 2022. Comprehensive evaluation of a high-temperature resistant re-crosslinkable preformed particle gel for water management. Fuel 309, 122086. https://doi.org/10.1016/j.fuel.2021.122086.

Zhang, H., Yang, H., Sarsenbekuly, B., Zhang, M., Jiang, H., Kang, W., Aidarova, S., 2020. The advances of organic chromium based polymer gels and their application in improved oil recovery. Adv. Colloid Interface Sci. 282, 102214. https://doi.org/10.1016/j.cis.2020.102214.

Zhu, D., Bai, B., Hou, J., 2017a. Polymer gel systems for water management in high-temperature petroleum reservoirs: A chemical review. Energy Fuels 31 (12), 13063–13087. https://doi.org/10.1021/acs.energyfuels.7b02897.

Zhu, D., Hou, J., Wei, Q., Wu, X., Bai, B., 2017b. Terpolymer gel system formed by resorcinol–hexamethylenetetramine for water management in extremely high-temperature reservoirs. Energy Fuels 31 (2), 1519–1528. https://doi.org/10.1021/acs.energyfuels.6b03188.

Zhu, D., Hou, J., Wei, Q., Chen, Y., 2019. Development of a high-temperature-resistant polymer-gel system for conformance control in Jidong oil field. SPE Reservoir Eval. Eng. 22 (1), 100–109. https://doi.org/10.2118/186235-PA.

Zhu, D.Y., Deng, Z.H., Chen, S.W., 2021. A review of nuclear magnetic resonance (NMR) technology applied in the characterization of polymer gels for petroleum reservoir conformance control. Pet. Sci. 18 (6), 1760–1775. https://doi.org/10.1016/j.petsci.2021.09.008.

Zhu, D., Zhang, H., Gao, Y., Zhang, J., Wang, Y., Liu, Y., 2024. Development of nanomontmorillonite-reinforced terpolymer gels for high-temperature petroleum reservoirs. Energy Fuels 38 (10), 8579–8588. https://doi.org/10.1021/acs.energyfuels.4c00655.

Zhu, D.Y., Zhang, J., Zhang, T., Gao, Y., Guo, S., Yang, Y., Lu, J., 2025. Damage mechanism analysis of polymer gel to petroleum reservoirs and development of new protective methods based on NMR technique. Pet. Sci. 22 (3), 1225–1233. https://doi.org/10.1016/j.petsci.2024.12.004.